Hindawi
Advances in Civil Engineering
Volume 2021, Article ID 8831778, 13 pages
https://doi.org/10.1155/2021/8831778

Research Article

Numerical Study on Soft Coal Pillar Stability in an Island Longwall Panel

Qingyun Xu[1,2], **Jian-Biao Bai**[1,3], **Shuai Yan**[1], **Rui Wang**[1] and **Shaoxu Wu**[4]

[1]*State Key Laboratory of Coal Resources and Safe Mining, School of Mines, China University of Mining and Technology, Xuzhou, Jiangsu 221116, China*
[2]*School of Coal Engineering, Shanxi Datong University, Datong, Shanxi 037003, China*
[3]*Institute of Mining Engineering and Geology, Xinjiang Institute of Engineering, Urumqi, Xinjiang 830091, China*
[4]*Beijing Research Institute of Uranium Geology, Beijing 100029, China*

Correspondence should be addressed to Jian-Biao Bai; baijianbiao@cumt.edu.cn and Shuai Yan; yanshuai@cumt.edu.cn

Received 13 March 2020; Revised 27 December 2020; Accepted 15 January 2021; Published 30 January 2021

Academic Editor: Ting-Xiang Chu

Roadway support and management of longwall panels in an island soft coal panel are always difficult work. In a test mine, stress distribution, deformation characteristic, and plastic zone distribution around the roadway and coal pillars in the development and mining periods were investigated with respect to the widths of different coal pillars using theoretical and simulation methods. The most reasonable width of coal pillars was comprehensively determined, and the field test was conducted successfully. The results show that a reasonable width of coal pillars is 7.0–8.2 m using the analytical method. The distribution of vertical stress in the coal pillars showed an asymmetric "double-hump" shape, in which the range of abutment pressure was about 26.0–43.0 m, and the roadway should be laid away from stress concentration. When the coal pillar width is 5.0–7.0 m, deformation of the roadway is half that with 8.0–10.0 m coal pillar in the development and mining period. The plastic zone in the surrounding rock firstly decreases and increases with increasing coal pillar width; the smallest range occurs with a coal pillar width of 5.0 m. Finally, a reasonable width for coal pillars in an island panel was determined to be 5.0 m. Industrial practice indicated that a coal pillar width of 5.0 m efficiently controlled deformation of the surrounding rock, which was an important basis for choosing the width of coal pillars around gob-side entries in island longwall panels with similar geological conditions.

1. Introduction

Gateway support of the island longwall panel in the soft coal seam is always a difficult problem because of stress concentration, which leads to serious deformation and failure of the surrounding rock and threatens the safety production [1, 2]. Besides, the strata behavior is more severe in the soft coal seam, so the influence of mining and side abutment pressure is more obvious in the island longwall panel inside of the soft coal seam, especially in the gob-side entry [3–6]. These characters highlight the support problem in safety production and construction of the coal mine.

In recent years, a series of research on the stress and yield behavior of the coal pillar in the island longwall panel has been studied, including the study methods, the formula to calculate the reasonable width of the coal pillar, and the control mechanism of the surrounding rock [7–12]. However, these studies are mostly based on soft rock roadway or ordinary island panel, respectively, and those aiming at the coal pillar width and surrounding rock control of the gob-side entry in the island panel inside of the soft coal seam are less. Island panel in the soft coal seam is a special kind of mining roadway [13–15]. Different from the deformation mechanism of the surrounding rock in ordinary conditions, the coal quality around the roadway is very fragile, and the mechanical environment is complex; moreover, stress concentrates in the island panel, and high abutment pressure appears in the gob-side entry with the influence of side abutment pressure and superimposed advance stress, distributing asymmetrically in both sides [16–18].

Combining the practical conditions of the longwall panel #7221 in the Jiegou mine, according to the study on reasonable coal pillar width based on stress distribution law and deformation and failure characteristics, this article provides an important basis for choosing the reasonable support methods and parameters, proposing efficient control measures and holding the support technology of mining roadway in the island panel with similar geological conditions.

2. The Coal Pillar Stability around the Gob-Side Entry in an Island Panel

2.1. The Structure of Overlying Strata in the Island Panel. In the mining period of the adjacent longwall panel, the immediate roof collapses completely and fills the goaf, and the main roof forms a stable structure—"voussoir beam," as shown in Figure 1(a) [19–22]. According to the cause of the "voussoir beam" and the extraction influence of adjacent working force, cracks appear and evolve in block A which is located in the overlying strata of longwall panel, while block C directly loads its weight on the collapsed immediate roof on goaf because of the effect of mining and filling. Therefore, an inclined arc triangle block B is formed between goaf and unexploited coal, and the stability of block B mainly depends on the hinge joint 2 on unexploited coal and hinge joint 1 on goaf. The structure of the "voussoir beam" can not only bear overlying rock seam but also decrease the load on subjacent coal, and then, the coal pillar around the gob-side entry can avoid overmuch fracture and failure caused by overload [23–25].

In the extraction period of this longwall panel, the immediate roof collapses and fills the goaf and the main roof breaks, so the forming block D directly loads its weight on fallen gangue. At the same time, because of the combined effect of the formation of the "voussoir beam" in the previous panel, the load bearing of the hinge joint 2, hinge joint 3, and coal pillar, the block A is embedded on the top of goaf, just like block B. Therefore, a "spatial three-hinged arch" coupled by two "voussoir beams" forms on the top of the coal pillar, as shown in Figure 1(b).

2.2. The Pillar Stress Distribution. The stress distribution law of the coal pillar with different widths is analyzed by numerical calculation, as shown in Figure 2. It can be included that ① the single peak of stress contribution is closer to the gob side of the coal pillar instead of in the center position, and the deviation distance is about 0.3–0.5 m; ② overall, the vertical stress is highest in the coal pillar, while the horizontal stress parallel to the axial direction of the roadway is lower, and the horizontal stress vertical to the axial direction of roadway is lowest; ③ when the coal pillar width is relatively small, like 4 m, influenced by the extraction and roadway driving of the previous panel, the coal pillar fractures seriously and relieves the pressure, so the vertical stress and horizontal stress are both lower than original rock stress; as the coal pillar width increases, the vertical and the horizontal stress parallel to the axial direction of roadway concentrate, so the stress in the center of the pillar is higher than original rock stress, while the horizontal stress vertical to the axial direction of roadway is lower; ④ in every coal pillar with different widths, the range of where vertical stress is lower than original rock stress is 4.0–4.6 m, and therefore, in similar geological conditions, the total range of the fracture zone in the narrow coal pillar is 4.0–4.6 m, in which the fracture range of the roadway side is about 2.0–2.6 m, and that of the gob side is about 2.0 m.

2.3. The Bearing Capacity of the Coal Pillar. The stability and maintenance of the narrow coal pillar are closely related to pillar width and support method. The reasonable width of the coal pillar has been studied according to field practice, theoretical analysis, limit equilibrium theory, elastic-plastic theory, and numerical analysis, respectively, and the theory and empirical formula for width determination were proposed, which indicates that a certain width of the elastic bearing core is needed to maintain the stability of the coal pillar. However, in a narrow coal pillar, influenced by side abutment pressure of stope, the plastic zone is widely contributed in the coal pillar. Therefore, the main problem in the gob-side entry with the narrow pillar is how to stabilize the plastic coal pillar.

According to the limit equilibrium theory, the narrow pillar which is located in the side abutment stress zone is filled with the fracture zone and plastic zone, and no elastic bearing zone. The coal pillar deformation is large under relatively small stress, and generally, this kind of pillar is hard to support because of extremely low stability and bearing capacity. But as the narrow pillar is mostly situated in the low bearing environment, it can be stable if some proper support measures are taken to increase the width and bearing capacity of the stable limit plastic zone inside of the coal pillar.

3. Geological and Industrial Conditions

The longwall panel #7221 is located in the first mining district and the #7 coal seam is located in the Jiegou mine, with an auxiliary uphill rise entry in the left and a coal pillar for the DF11 fault in the right. The adjacent longwall panels, #7220 and #7222, have been mined out. The mining seam in the longwall panel #7221 is 4.8 m thick (3.5–6.12 m) and dips 6° (9°–16°) on average. The strike length is 960 m, and the dip length is 100–157 m. The gob-side entry is excavated along the roof of the #7 coal seam. The conditions of the coal seam, roof, and floor can be seen in the synthesis column map (Figure 3).

4. Theoretical Calculation of Coal Pillar Width

4.1. The Width Determined by Limit Equilibrium Theory. At the edge of goaf in the longwall panel #7222, there are three stress zones under the arc triangle block in the main roof. To ensure the stability of the machine entry of the longwall panel #7222, the entry must be arranged in the stress decreasing zone in the internal side of the coal wall. The width of the protective pillar can directly influence

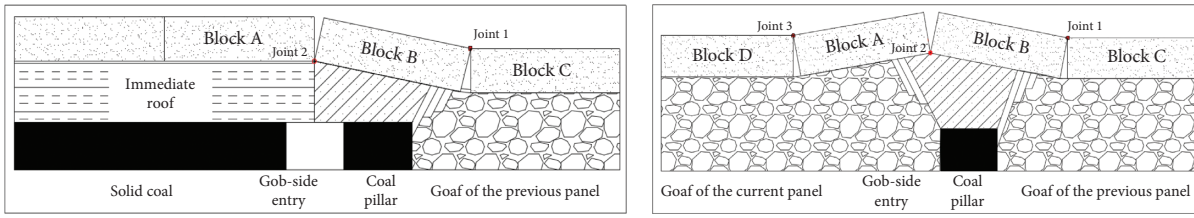

Figure 1: Structure model of overlying strata in the gob-side entry. (a) The fracture model of the main roof in the adjacent face. (b) The fracture model of the main roof in this face.

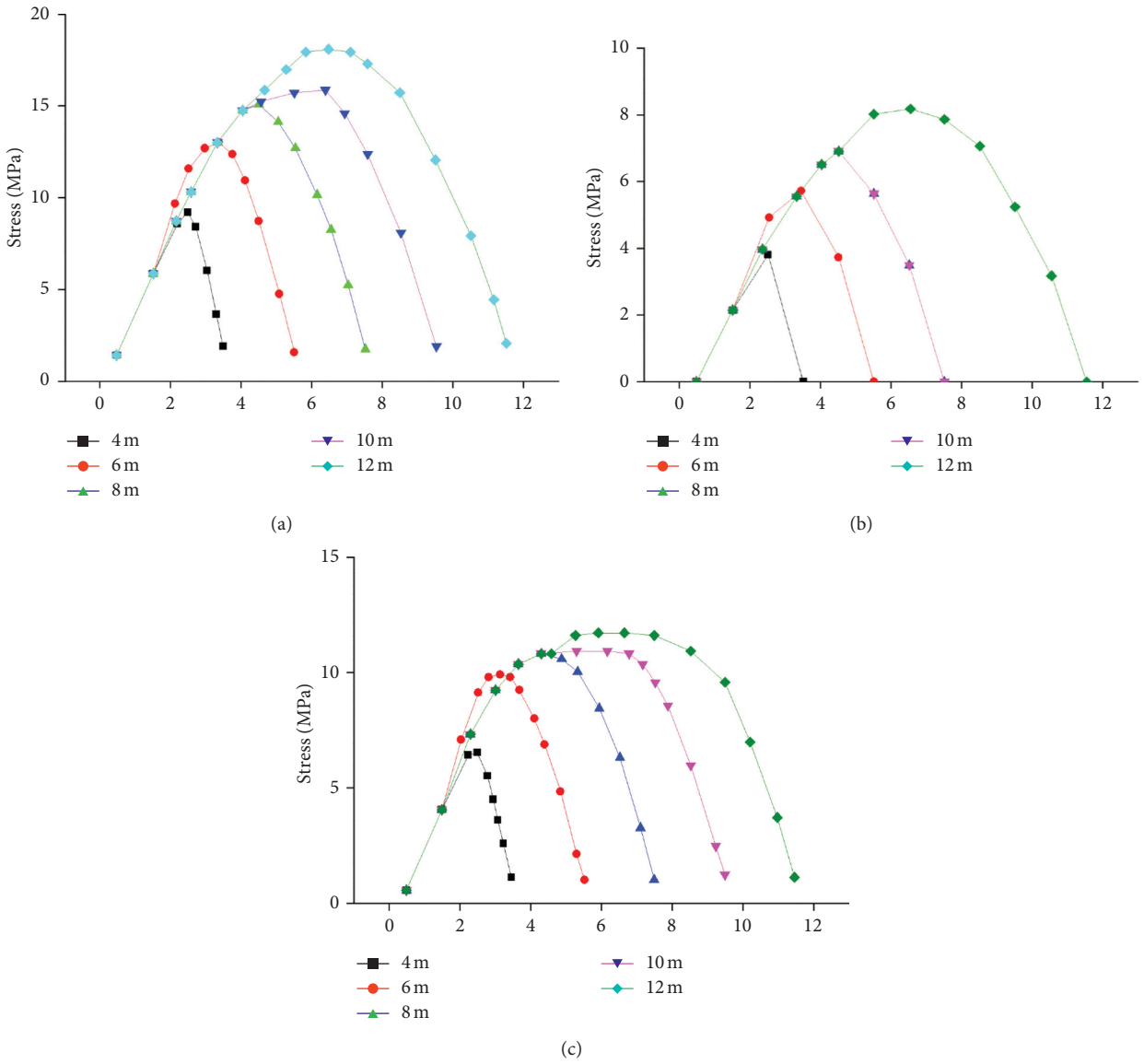

Figure 2: Stress distribution of the coal pillar in the gob-side entry. (a) Vertical stress. (b) Horizontal stress vertical to the axial location of the roadway. (c) Horizontal stress of the axial location of the roadway.

coal mining rate and pillar stability (two mutually contradictory factors): too wide coal pillar will decrease the coal mining rate, while too narrow coal pillar will lead to large deformation and serious fracture of the coal body and increase the difficulty of maintenance, or even cause air leakage and threaten the safety production. The reasonable coal pillar width can be calculated as shown in Figure 4.

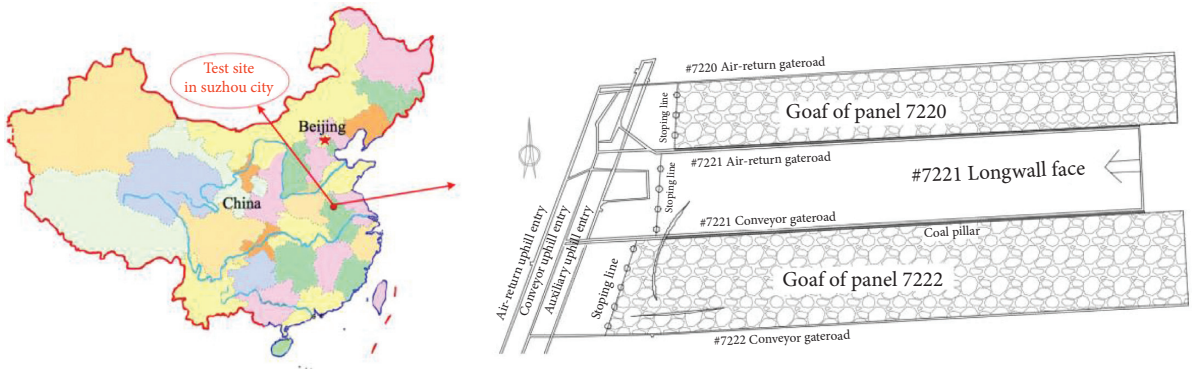

Figure 3: Mine location and layout drawing of the experimental roadway.

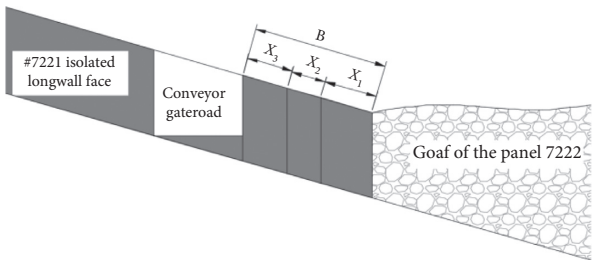

Figure 4: The calculation of coal pillar width.

X_1 can be calculated by the following formula:

$$X_1 = \frac{mA}{2\tan\varphi_0}\ln\left(\frac{K\gamma H + (C_0/\tan\varphi_0)}{(C_0/\tan\varphi_0) + (P_z/A)}\right), \quad (1)$$

where m is the thickness of the coal seam, A is the side pressure coefficient ($A = 0.49$), calculated by $A = \mu/(1-\mu)$ ($\mu = 0.33$, the Poisson ratio), φ_0 is the internal friction angle of the coal seam (18°), C_0 is the cohesion of the coal seam (0.58 MPa), K is the stress concentration factor (2.0), γ is the average bulk density of the rock (24 kN/m^3), H is the depth of the roadway (350 m), and P_z is the support resistance of the stent ($Pz = 0$ because these stents are in the gob side).

$$X_3 = \left(\frac{K\gamma HB}{10^4 f_y} - 1\right)h\tan\frac{90^\circ - \phi_0}{2}, \quad (2)$$

where B is the dimensionless parameter to characterize the extent of mining influence (1.5), f_y is the hardness ratio of the coal seam (0.41), and h is the thickness of the coal shed in the roadway (2.8 m). The other parameters are the same as those in equation (1).

$$X_2 = (X_1 + X_3)(20\% \sim 40\%), \quad (3)$$

where X_1 is the plastic zone width of gob, X_2 is the elastic zone width, and X_3 is the plastic zone width of the coal pillar. According to the above conditions, it can be calculated as follows: $X_1 = 4.27$ m and $X_3 = 1.7$ m, and then, $X_2 = 1.17$–2.35 m, and finally, $B = 7.0$–8.2 m.

Because coal pillar instability is mainly triggered by the evolution of the fracture quantity in the coal pillar, coal pillar changed from the stable state into the unstable failure state. Both X_1 and X_3 are maximum widths of plastic zones on both sides of the coal pillar obtained by limit equilibrium theory. Meanwhile, the vertical stress distribution in the stable abutment coal pillar around the gob-side entry is saddle-shaped. When the coal pillar transits from stable to yield state, vertical stress distribution is hump-shaped. In the analysis model of the stability mechanism of the coal pillar, the width of the fracture zone is larger than that of the coal pillar. The width of the plastic zone is larger, and the possibility of instability is bigger.

In accordance with ultimate strength theory, the safety factor of the coal pillar is as follows:

$$f = \frac{\sigma_z(X_1 + X_2 + X_3)}{\gamma H(X_1 + X_2 + X_3 + L_E)}, \quad (4)$$

where L_E is the width of the gateroad.

The safety factor of the coal pillar is generally more than 1.3. Meanwhile, the coal pillar stress law shows that failure width exceeds 35% width of the coal pillar, and the coal pillar will have instability failure. Therefore, to keep the supporting coal pillar stable, two conditions for coal pillar stability must be satisfied at the same time. Firstly, the safety factor of the coal pillar is proper, and secondly, failure width of the coal pillar is not beyond its critical value.

4.2. The Width Determined by Internal-External Stress Field Theory. According to the internal-external stress fields theory [16], the abutment stress delivered from overlying rock strata to the coal body can be divided into 2 parts by the fracture line when the main roof failed: S1, the internal stress field between the fracture line and coal wall in goaf, and S2, the external stress field between the fracture line and deep region [26]. The internal stress field can be calculated by the following formula:

$$S_1 = \sqrt{\frac{LL_2S_Ph_Z}{(L + L_2)KH}}, \quad (5)$$

where L_2 is the first weighting interval ($L_2 = 35$ m), L is the length of the longwall panel ($L = 230.5$ m), S_P is the influence scope of advanced abutment stress ($S_P = 40$ m), and h_z is the thickness of the arc triangle block ($h_z = 10.11$ m). Substitute

the value into equation (5), a result that is similar to equation (1) can be obtained.

5. Numerical Calculation of Coal Pillar Width

5.1. The Strain-Softening Model of the Coal Seam. For meeting the natural conditions and studying the mechanical parameters of the soft coal seam, numerical simulation software Flac3D was adopted, and the strain-softening model was used for the uniaxial compression simulation experiment, and the experiment results that fit the curve concluded by the laboratory test were obtained accordingly to adjust the mechanical parameters of this model, such as cohesion and internal friction angle [27–31]. Finally, the most reasonable simulation parameters were determined. The fitting comparison curve of stress-strain is shown in Figure 5.

By comparing the stress-strain curves by the simulation experiment and laboratory test, concrete parameters of the strain-softening model are obtained, as shown in Table 1. The parameters of the coal seam for the model are indicated in Table 1.

5.2. Global Model and Simulation Plans. To ensure the safe extraction of the present longwall panel (the roadway is stable and can be used during the roadway driving period and extraction period), in terms of the natural geological conditions of the #7221 island longwall panel, the conveyor entry is chosen as the research object to build the numerical model and to study the influence of the coal pillar with different widths on the surrounding rock deformation of the gob-side entry. The boundary constraint conditions of the model with dimensions of 209 m long × 80 m wide × 119.7 m high can be seen in Figure 6, in which the load is calculated with the mining depth of 3103 m, and the side pressure coefficient is 1.2. The size of the roadway section in the simulation is 4.5 m × 3.5 m, where 3.5 m is the average height of the oblique trapezoid.

The calibrated input parameters for the strain-softening model are shown in Table 2. Therefore, the input parameters in Table 2 can be used to simulate the strain-softening behavior of the surrounding rock.

In the numerical simulation, the Mohr–Coulomb's criterion is adopted to estimate the failure of the surrounding rock in the whole model, except the coal seam wherein the strain-softening model is used [32, 33]. Combing the field measurement and theoretical calculation, 5 models with the coal pillar of different widths (3 m, 5 m, 7 m, 8 m, and 10 m) are built. According to the study, the stress distribution and change of the coal pillar in the front and back of the longwall panel, which advances 50 m, the formation of the island longwall panel, the driving of conveyor roadway, and the mining process are simulated.

6. Global Model Results

6.1. Stress Analysis of the Longwall Panel. The stress distribution is analyzed in the period after the stabilization of goaf in both sides and before the roadway driving of the present

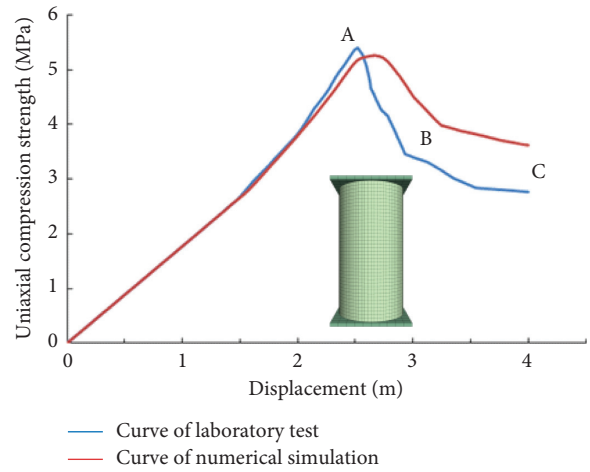

Figure 5: Contrast diagram of the stress-strain curve between numerical simulation and laboratory test.

Table 1: Parameters of the soft coal seam for the strain-softening Mohr–Coulomb.

Strain (mm)	Cohesion (MPa)	Internal friction angle (°)
0	2.9	21
0.01	1.8	19
0.02	1.1	18
0.03	0.7	16
1	0.4	16

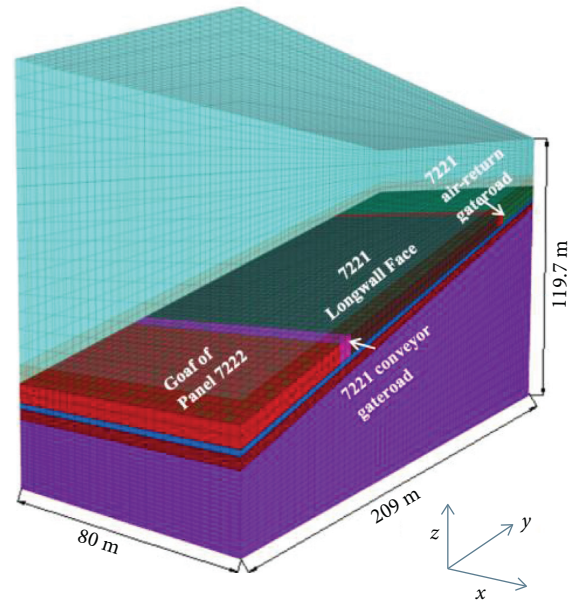

Figure 6: Numerical calculation model.

longwall panel. The stress nephogram in the longwall panel can be seen in Figure 7. When the coal pillar width is 7 m, the distribution of internal vertical stress along the coal seam is indicated in Figure 8.

The following can be concluded from Figures 7 and 8: after the exploitation of adjacent longwall panels, the

Table 2: The mechanical parameters of the surrounding rock.

Lithology	Thickness (m)	Bulk K (GPa)	Shear G (GPa)	Internal friction angle f (°)	Cohesion C (MPa)	Tensile strength t (MPa)
Medium sandstone	6.05	25.2	15.0	30	3.0	1.5
Fine sandstone	4.24	20.2	10.0	35	2.4	4.13
Mudstone	3.16	6.2	4.0	22	0.6	0.15
# 7 coal seam	2.5	2.0	0.75	33	0.6	0.2
Shaly sandstone	1.3	7.0	5.0	24	1.0	1.0
Siltstone	6.73	12.3	9.0	30	1.2	1.5
Fine sandstone	7.97	20.2	10.0	35	2.4	4.13
# 8 coal seam	2.4	3.57	0.71	25	0.56	0.49
Carbonaceous mudstone	4.96	6.2	4.0	30	0.8	0.15
Siltstone	2.92	12.3	9.0	40	2.4	1.51
Medium sandstone	3.5	25.2	15.0	30	3	1.5

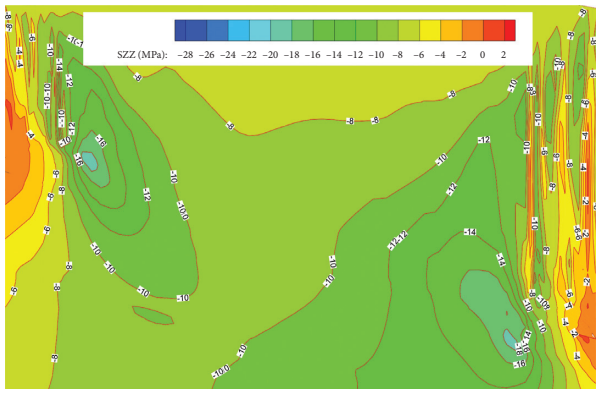

Figure 7: Distribution of abutment pressure in the gob side of the soft coal seam.

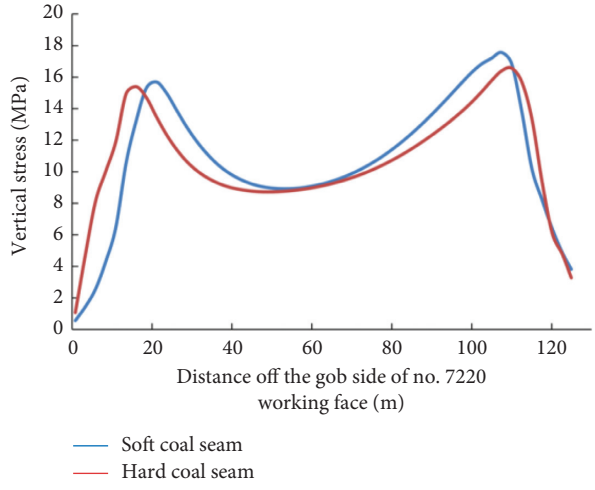

Figure 8: Distribution curve of vertical stress in gob sides in the island longwall panel.

distribution of side abutment pressure cannot overlap inside of the longwall panel area because of large width; however, because by the soft coal seam, the influence area of side abutment pressure and fracture zone of the coal body is relatively large, and the original rock stress zone fills the coal pillar that is 40–75 m off the next panel. The distribution of vertical stress in the longwall panel exhibits an asymmetric "saddle shape." In the range of 0–12 m off the goaf of the previous panel, about 12 m, the stress decreases. In the range of 12–38 m, about 26 m, the stress increases and the peak value is 15.8 MPa, located 22 m off the goaf. The original rock stress zone is in the range of 38–72 m, and the stress increases in the range of 72–115 m in where the peak value is 17.6 MPa, located 105 m off the goaf. Finally, in the range of 115–125 m, the vertical stress decreases. Inferred from the above conclusions, the range of the stress decreasing zone in the island longwall panel inside of the soft coal seam is twice as large as that inside of the hard coal seam, and the stress peak is closer to the longwall panel, which can influence the determination of coal pillar width because of the low bearing capacity of the soft coal body. Moreover, the range of the overstressed zone does not change a lot, while the in situ stress zone is smaller in the island longwall face.

6.2. Stress Distribution Law of the Coal Pillar. The stress distribution law of the coal pillar is analyzed in the roadway driving period and extraction period. This article is focusing on the stress distribution of coal pillar and unexploited coal in the range of 55 m off the roadway, and these data are all collected from the center of the pillar. Figure 9(a) indicates the stress distribution curve of the coal pillar along the horizontal direction that is vertical to the roadway in the roadway driving period, and the stress distribution of the position that is 55 m before the longwall panel as the face advances 140 m in the extraction period is shown in Figure 9(b).

It can be seen in Figure 9(a) that, in the aspect of vertical stress, with the different widths of the coal pillar, the largest stress in the pillar is smaller than that in unexploited coal, while the stress amplification in the pillar is larger. Meanwhile, the stress curve changes slightly in the coal pillar with 3–5 m width but fluctuates in the 7–10 m pillar. As to horizontal stress, after the roadway driving, the stress distributes gently in the coal pillar with 3–5 m width, and the value is relatively small without noticeable peak, while in the 7–10 m pillar, the obvious stress peak occurs and increases largely. Overall, during the period of roadway driving, the stress distribution curve, increasing as the coal pillar width

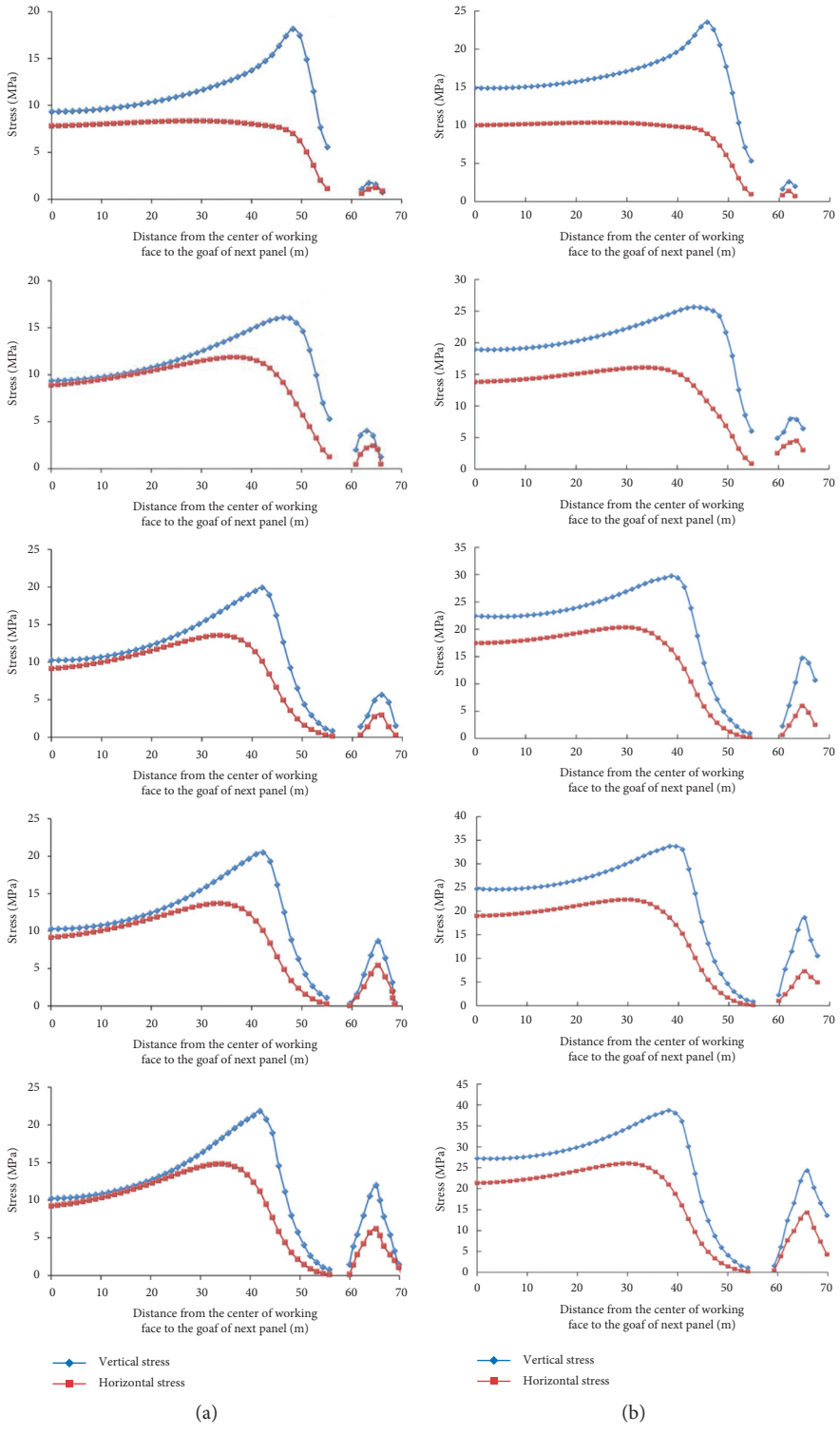

Figure 9: Stress distribution of different coal pillars during roadway driving and extraction periods. (a) The roadway driving period. (b) The extraction period.

rises, is similar to the deformation and failure characteristics of the rock and changes as an isosceles triangle. The vertical stress changes more obviously than horizontal stress, and in the unexploited coal, the horizontal stress changes slightly, compared to vertical stress. Moreover, with the increase of coal pillar width, the influence area and peak value of side abutment stress in overlying rock strata of goaf grow gradually and threaten the roadway stability.

Concluded from Figure 9(b), in the aspect of vertical stress, the stress and peak value increases as the coal pillar

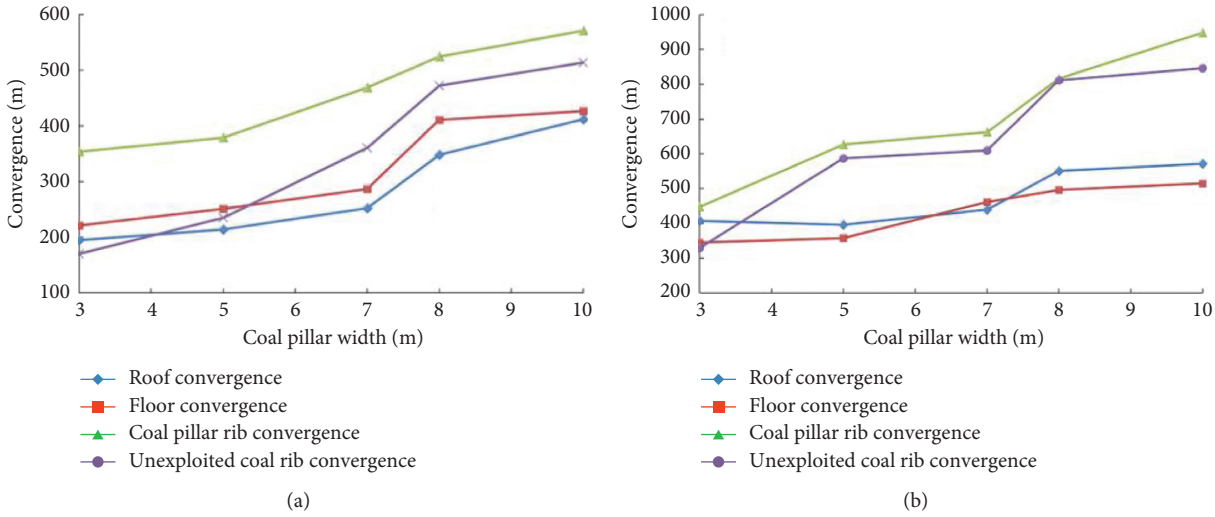

Figure 10: Relationship between the deformation of the surrounding rock and coal pillar width during roadway driving and extraction periods. (a) The roadway driving period. (b) The extraction period.

width rises, and the influence area of side abutment stress grows. When the width of the coal pillar is 3 m, 7 m, 8 m, and 10 m, the peak value is 23.5 MPa, 29.8 MPa, 33.7 MPa, and 38.7 MPa, respectively. However, the peak is not obvious, about 25.7 MPa, and the influence area is small as the coal pillar width is 5 m. As to horizontal stress, influenced by extraction, horizontal stress increases apparently, and the stress distributes gently without noticeable peak in the coal pillar with 3–5 m width, while in the 7–10 m pillar, the obvious stress peak occurs. Overall, during the period of extraction, the stress distributes similarly in the coal pillar with different widths, and compared to the roadway driving period, the stress value increases largely but changes more slightly. Meanwhile, the stress increases as the coal pillar width rises and exhibits an irregular triangle. The stress distribution curve changes gently when the coal pillar width is 3–5 m, while in the 7–10 m wide coal pillar, the stress peak is noticeable and concentrated.

Combining and comparing the characteristics of stress distribution in different periods, it can be concluded that when the coal pillar width is 5 m, the peak values and influence areas of vertical stress and horizontal stress are all relatively small in both sides of roadway. So, 5 m is the reasonable width.

6.3. Deformation Characteristics of the Surrounding Rock. According to the study on the deformation of the coal pillar during the roadway driving period and extraction period, the reasonable coal pillar width is determined. The deformation of the middle part with half of coal pillar height along the horizontal direction that is vertical to roadway is analyzed, and the curve that characterizes the relationship between coal pillar width and deformation of the surrounding rock is concluded, as shown in Figure 10.

From Figure 10(a), it can be seen that when the coal pillar width is 3–7 m, the stability of the coal pillar is relatively high, and the vertical displacement is small, and when the width is 3–5 m, the horizontal displacement is small and gentle, while it increases largely as the coal pillar width rises to 7 m. When the width is 8 m, the surface displacement of the roadway increases rapidly, and the deformation is noticeable. And when the width rises to 10 m, all of the deformation parameters reach the peak. Overall, the vertical displacement is smaller than the horizontal displacement and changes smoothly. Therefore, considering the surface displacement of the roadway during the driving period, the reasonable width of the coal pillar is 5 m.

From Figure 10(b), it can be concluded that when the coal pillar width is 3 m, the surface displacement in whole roadway is alike, about 400 mm, but the coal pillar, with failure inside, has a low bearing capacity. When the coal pillar width is 5–7 m, the convergence of the coal pillar is larger than that of unexploited coal, and the roof-to-floor convergence of roadway is almost the same but has increased noticeably compared with that in the 3 m coal pillar. When the coal pillar width is 8–10 m, surface displacement of roadway increases and rib-to-rib convergence changes rapidly, and the roadway deformation is serious. All the parameters of the convergence tend to be stable except the convergence of the coal pillar. Therefore, considering the surface displacement of roadway during the extraction period, the reasonable width of the coal pillar is 5 m.

6.4. Distribution Law of the Plastic Zone. It can be concluded from Figure 11 that the failure areas that are affected by the coal pillar with different width in the plastic zone are different too. Due to the influence of adjacent goafs and present roadway driving, the internal coal pillar and surrounding rock of roadway are affected, and the unexploited coal turns to the plastic zone, but the internal longwall panel is in the elastic state. When the coal pillar width is 3 m, tension and shear fractures have appeared, and the unexploited coal rib in the range of 12 m has been sheared or is being sheared, and most of the roof has been sheared too. When the coal

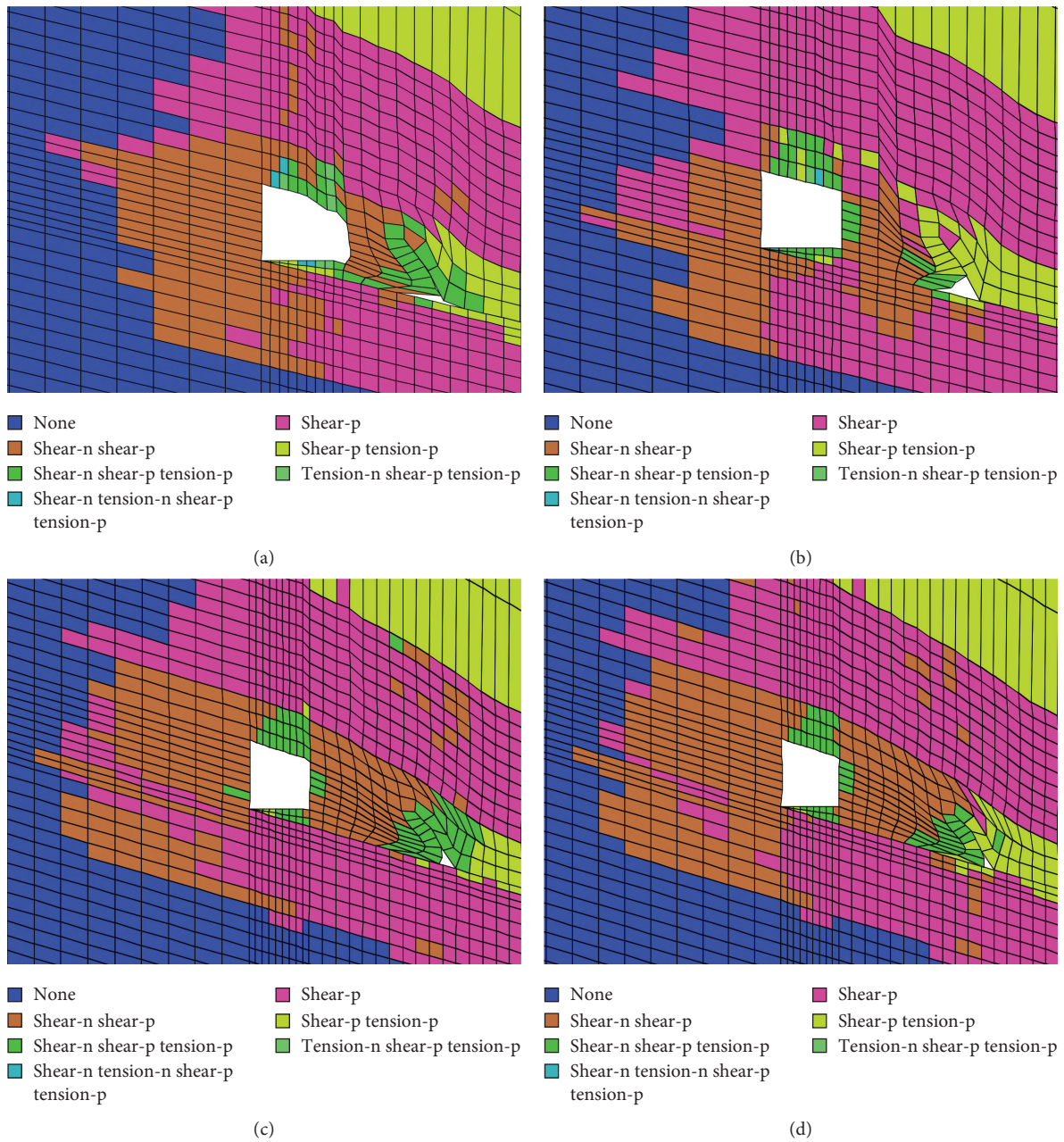

Figure 11: Continued.

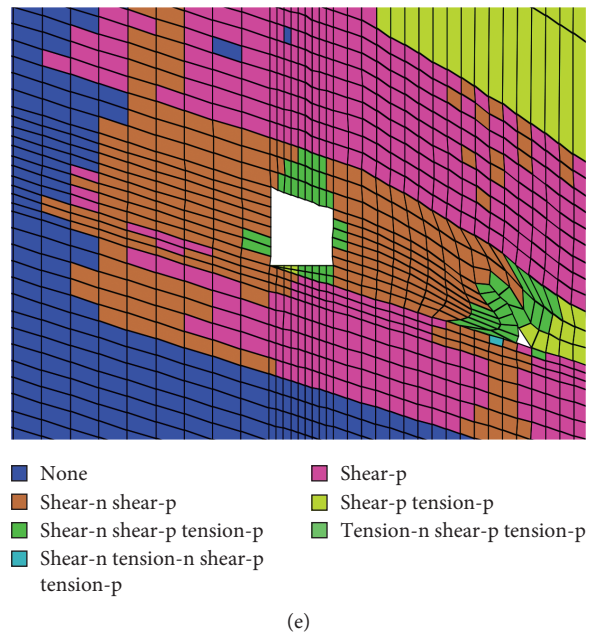

Figure 11: Distribution of the plastic zone in the mining gateway with different coal pillar widths: (a) 3 m, (b) 5 m, (c) 7 m, (d) 8 m, and (e) 10 m.

pillar width is 5 m, the fracture zone declines in the rib of unexploited coal, and the failure of the coal pillar is dominated by shear fracture, and the failure area in the roof increases. When the coal pillar width is 7-8 m, the unexploited coal rib in the range of 14 m is sheared to different extents, and tension fracture appears in the roof, floor, and coal pillar. When the coal pillar width is 10 m, the failure area in unexploited coal rises to 16 m, and the tension fracture zone in the surrounding rock increases too; as to roof, the shear fracture zone is more extensive and further breaks the roof. Overall, the tension fracture zone in different extent appears in the surrounding rock, and the failure area in the unexploited coal rib rises as the coal pillar width increases as well as in the roof, while the plastic zone changes slightly in the floor. Therefore, when the coal pillar width is 5 m, the plastic zone is smallest, and the surrounding rock is most stable.

6.5. Determination of Coal Pillar Width. According to theoretical calculation, stress distribution and deformation characteristics in the island longwall panel, and plastic zone distribution in extraction roadway, combining the stress distribution characteristics in the soft coal seam and increase of the mining rate, the reasonable width of the protective coal pillar in the island longwall panel inside of the soft-coal seam is determined to be 5 m.

7. Field Test

This study optimized the original support scheme and proposed new support schemes that fit different periods and positions. The field test is implemented in the conveyor entry of the #7221 longwall panel. In the test roadway, three stations are arranged to measure the roof-to-floor convergence, coal pillar rib convergence, and unexploited coal rib convergence in the same section during different periods, respectively.

7.1. Analysis of the Support Situation during the Roadway Driving Period. In this paper, displacement monitoring of the entry surface and fracture zone monitoring using borehole imaging were employed to monitor roadway deformation during entry development and panel retreat [34, 35]. The convergence station consisted of permanent pins (red solid circles in Figure 12) installed in the roof, floor, yield pillar rib, and solid coal rib. A portable telescopic rod (Figure 12(a)) and measuring lines were used to record the roof and floor convergences, and the rib convergence was measured using a flexible tape and measuring lines. The exploratory borehole drilled in the entry was used to obtain video footage of fracture development using a borehole imaging tool (Figure 12(b)). Specialist technicians performed all measurements.

According to the observation in 3 months during the roadway driving period, these results in each station are close, in which the result in the #2 station is shown in Figure 12.

It can be seen from Figure 13 that, overall, after the combined support during the driving period, the convergence of rib to rib is larger than that of roof to floor, and deformation of the coal pillar rib is larger than that of the unexploited coal rib. The largest convergence of roof to floor, coal pillar rib, unexploited coal rib, and rib to rib is 523 mm, 488 mm, 261 mm, and 749 mm, respectively.

Figure 14 shows the internal conditions of the yield pillar in monitoring station #3. Photographs were obtained using

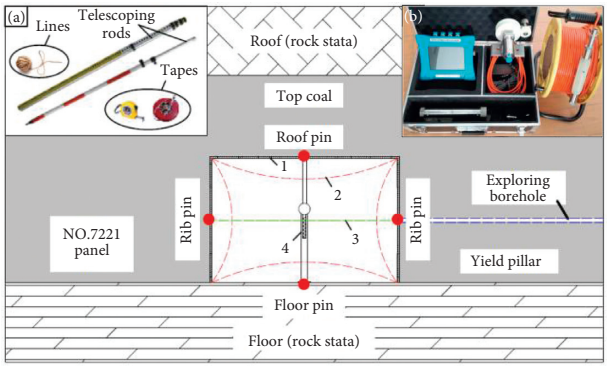

FIGURE 12: Borehole camera exploration and portable telescopic rod in the monitoring station.

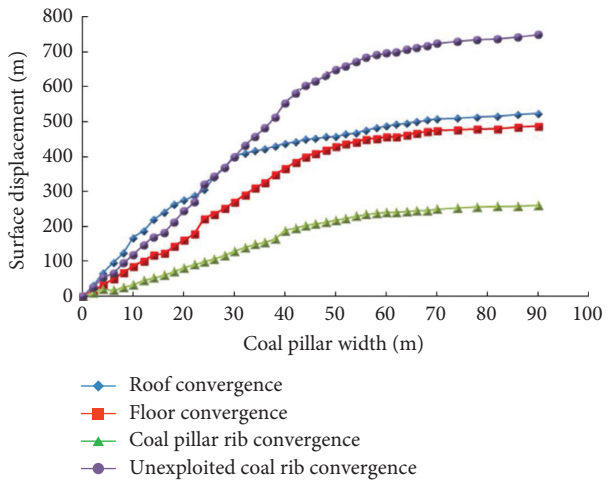

FIGURE 13: Surface displacement curve of the #2 station during the roadway driving period.

the penetrating video on the wall of a horizontal borehole drilled into the yield pillar (see Figure 12). It can be seen from Figure 14 that the coal mass close to the yield pillar rib has severely failed, and massive fractures are present in the internal coal mass of the yield pillar. The yield pillar has, therefore, been completely fragmented. Hence, we have every reason to believe that the yield pillar had completely entered into a yielding state after entry development.

The convergence of the coal pillar rib is about 1.8 times that of the unexploited coal rib, and the rib-to-rib convergence, tending to be stable after 45 days, is about 1.4 times as the roof-to-floor convergence that stabilizes after 32 days. Supported by the original scheme, the convergence of roof to floor and rib to rib is 1480 mm and 1670 mm, respectively, while those parameters under the optimized support scheme decline by 59.5% and 48.5%, respectively.

7.2. Analysis of the Support Situation during the Roadway Extraction Period. During the extraction period, the convergence of roof to floor and rib to rib increases by 30.0% and 33.8%, respectively, compared with the roadway driving period, and due to the influence of advanced abutment stress

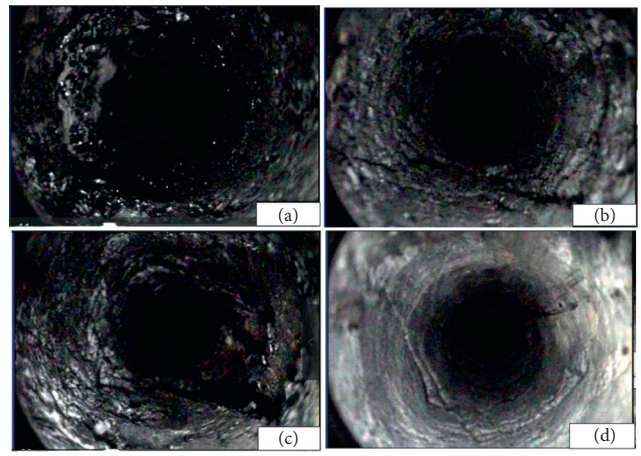

FIGURE 14: Still photographs from video footage obtained from a borehole drilled in the yield pillar. (a) 1.0 m, (b) 3.0 m, (c) 2.0 m, and (d) 4.0 m.

and fracture of the surrounding rock, the deformation becomes serious as the longwall panel advances and closes to the station. The deformation of the surrounding rock is large in the range of 80 m off the longwall panel, but the deformation is acceptable, and some measures like tunnel bottom and reinforce support can be adopted to maintain the normal production and transportation, while out of the range, the deformation is relatively small, and the surrounding rock is stable.

8. Conclusion

For the particularity of deformation in the soft coal seam, the strain-softening model is adopted as the constitutive model of numerical simulation, and fitting and comparing the curves obtained by numerical simulation and laboratory test determine specific parameters of this model. The results indicate that, due to the inclined soft coal seam, the affected area in an island longwall panel influenced by side abutment stress of adjacent goaf increases and internal vertical stress distributes as an asymmetric "saddle shape." The range of the stress increase zone near the return airway and the conveyor entry is 26.0 m and 43.0 m, respectively. Compared to the hard coal seam, the range of the stress decrease zone is larger in the soft coal seam, while the position of the stress peak is closer to the island longwall panel, which has a huge influence on the width determination of the coal pillar. According to theoretical calculation and analysis of the stress distribution law during different periods by numerical simulation as well as deformation characteristics and plastic zone distribution of roadway and coal pillar, the width of the coal pillar in the soft coal island longwall is finally determined to be 5.0 m.

The field test shows that, during the roadway driving period, the convergence of rib to rib was larger than that of roof to floor, about 1.4 times, and deformation of the coal pillar rib was larger than that of the solid coal rib, about 1.8 times. The roof-to-floor convergence came to be stable after 32 days, while the rib-to-rib convergence stabilized after 45

days. During the extraction period, the deformation became serious (the slope of the curve rises) as the longwall panel advances and closes to the station, and the range of the influence zone was about 80.0 m. Practice indicates that the coal pillar with 5.0 m can efficiently control the deformation of the surrounding rock and ensure the safety production.

Data Availability

The underlying data supporting the results of this study can be found by requesting the corresponding author.

Conflicts of Interest

The authors declare that they have no conflicts of interest.

Acknowledgments

This research was supported by the National Natural Science Foundation of China (Grant nos. 52074239 and 51927807).

References

[1] F. Carr, E. Martin, and B. H. Gardner, "How to eliminate roof and floor failures with yield pillar," *Coal Mining Process Part II*, vol. 21, pp. 44–49, 1985.

[2] W.-D. Wu, J.-B. Bai, X.-Y. Wang, S. Yan, and S.-X. Wu, "Numerical study of failure mechanisms and control techniques for a gob-side yield pillar in the Sijiazhuang coal mine, China," *Rock Mechanics and Rock Engineering*, vol. 52, no. 4, pp. 1231–1245, 2019.

[3] Y. Wang, *Strata-pressure behavior in the condition of different coal pillar sizes in the caigou coal*, Ph.D. thesis, China University of Mining and Technology, Beijing, China, 2011.

[4] W. Li, J. Bai, S. Peng, X. Wang, and Y. Xu, "Numerical modeling for yield pillar design: a case study," *Rock Mechanics and Rock Engineering*, vol. 48, no. 1, pp. 305–318, 2015.

[5] B. A. Poulsen, "Coal pillar load calculation by pressure arch theory and near field extraction ratio," *International Journal of Rock Mechanics and Mining Sciences*, vol. 47, no. 7, pp. 1158–1165, 2010.

[6] G.-C. Zhang, F.-L. He, H.-G. Jia, and Y.-H. Lai, "Analysis of gateroad stability in relation to yield pillar size: a case study," *Rock Mechanics and Rock Engineering*, vol. 50, no. 5, pp. 1263–1278, 2017.

[7] S. Yan, J. Bai, X. Wang, and L. Huo, "An innovative approach for gateroad layout in highly gassy longwall top coal caving," *International Journal of Rock Mechanics and Mining Sciences*, vol. 59, no. 4, pp. 33–41, 2013.

[8] S. Yan, T. X. Liu, J. B. Bai, and W. D. Wu, "Key parameters of gob-side entry retaining in a gassy and thin coal seam with hard roof," *Processes*, vol. 6, no. 5, pp. 51–65, 2018.

[9] Z. Z. Zhang, W. J. Wang, S. Q. Li et al., "An innovative approach for gob-side entry retaining with thick and hard roof: a case study," *Technical Gazette*, vol. 25, pp. 1028–1036, 2018.

[10] G. C. Zhang, Z. J. Wen, S. J. Liang et al., "Ground response of a gob-side entry in a longwall panel extracting 17 m-thick coal seam: a case study," *Rock Mechanics and Rock Engineering*, vol. 53, no. 2, pp. 497–516, 2019.

[11] G. Zhang, L. Chen, Z. Wen et al., "Squeezing failure behavior of roof-coal masses in a gob-side entry driven under unstable overlying strata," *Energy Science & Engineering*, vol. 8, no. 7, pp. 2443–2456, 2020.

[12] R. Wang, J.-B. Bai, S. Yan, Z.-G. Chang, and X.-Y. Wang, "An innovative approach to theoretical analysis of partitioned width & stability of strip pillar in strip mining," *International Journal of Rock Mechanics and Mining Sciences*, vol. 129, Article ID 104301, 2020.

[13] H. P. Kang, J. Lin, and M. J. Fan, "Investigation on support pattern of a coal mine roadway within soft rocks-a case study," *International Journal of Coal Geology*, vol. 140, pp. 31–40, 2015.

[14] I. B. Tulu, G. S. Esterhuizen, D. Gearhart, T. M. Klemetti, K. M. Mohamed, and D. W. H. Su, "Analysis of global and local stress changes in a longwall gateroad," *International Journal of Mining Science and Technology*, vol. 28, no. 1, pp. 127–135, 2018.

[15] Q. H. Qian, "The key scientific problems in the development of deep underground space," in *Proceedings of the 230th Xiangshan Science Conference*, Beijing, China, October 2004, in Chinese.

[16] W. J. Wang, C. J. Hou, and J. B. Bai, "Mechanical deformation analysis of the roof coal of road driving along next goaf in sublevel caving face," *Chinese Journal of Geo Technical Engineering*, vol. 23, no. 2, pp. 209–211, 2001.

[17] X. G. Zheng, Z. G. Yao, and N. Zhang, "Stress distribution of coal pillar with gob-side entry driving in the process of excavation & mining," *Journal of Mining & Safety Engineering*, vol. 29, no. 4, pp. 459–465, 2012.

[18] M. Wang, J. Bai, W. Li, X. Wang, and S. Cao, "Failure mechanism and control of deep gob-side entry," *Arabian Journal of Geosciences*, vol. 8, no. 11, pp. 9117–9131, 2015.

[19] J.-B. Bai, W.-L. Shen, G.-L. Guo, X.-Y. Wang, and Y. Yu, "Roof deformation, failure characteristics, and preventive techniques of gob-side entry driving heading adjacent to the advancing working face," *Rock Mechanics and Rock Engineering*, vol. 48, no. 6, pp. 2447–2458, 2015.

[20] Z. Z. Zhang, Z. T. Han, X. Y. Wang, and M. Wang, "Roof mechanics analysis and backfill technology for abandoned roadway," *Journal of Mining & Safety Engineering*, vol. 30, no. 2, pp. 194–198, 2013.

[21] E. Ghasemi, K. Shahriar, and M. Sharifzadeh, "A new method for risk assessment of pillar recovery operation," *Safety Science*, vol. 48, no. 10, pp. 1304–1312, 2010.

[22] E. Ghasemi, K. Shahriar, M. Sharifzadeh, and H. Hashemolhosseini, "Quantifying the uncertainty of pillar safety factor by Monte-Carlo simulation-a case study," *Archives of Mining Sciences*, vol. 55, no. 3, pp. 583–595, 2010.

[23] H. X. Fu, "Comments on differences between Kastner formula and Fenner formula used for plastic rock (soft rock)," *Journal of Railway Engineering Society*, vol. 22, no. 3, pp. 72–74, 2005.

[24] S. R. Xie, S. J. Li, Z Wei et al., "Stability control of support-surrounding rock system during fully mechanized caving face crossing abandoned roadway period," *Journal of China Coal Society*, vol. 40, no. 3, pp. 502–508, 2015.

[25] X. X. Chen, L. C. Wang, and D. H. Fu, "A study on inward movement deformation mechanism and control technology of dynamic pressure gateway of island mining face," *Journal of Mining & Safety Engineering*, vol. 32, no. 4, pp. 552–558, 2015.

[26] W. Gao, "The elastic-plastic analysis of stability of inclined coal pillar," *Mechanics and Practice*, vol. 23, no. 2, pp. 23–26, 2001.

[27] Y. N. Shi and H. F. Liu, "Determination of reasonable coal pillar width for roadway driving along gob in soft coal seam

with hard roof and soft floor," *Mining Safety & Environmental Protection*, vol. 43, no. 3, pp. 49–52, 2016.

[28] X. H. Li, M. H. Ju, S. K. Jia, and Z. H. Zhong, "Study of influential factors on the stability of narrow coal pillar in gob-side entry driving and its engineering application," *Journal of Mining & Safety Engineering*, vol. 33, no. 5, pp. 761–769, 2016.

[29] K. Jessu, A. Spearing, and M. Sharifzadeh, "Laboratory and numerical investigation on strength performance of inclined pillars," *Energies*, vol. 11, no. 11, p. 3229, 2018.

[30] F. K. Qi, Y. J. Zhou, Z. Z. Cao, Q. Zhang, and N. Li, "Width optimization of narrow coal pillar of roadway driving along goaf in fully mechanized top coal caving face," *Journal of Mining & Safety Engineering*, vol. 33, no. 3, pp. 475–480, 2016.

[31] X. Z. Hua, S. Liu, Z. H. Liu, W. H. Cha, and Y. F. Li, "Research on strata pressure characteristic of gob-side entry driving in island mining face and its engineering application," *Journal of Mining & Safety Engineering*, vol. 30, no. 8, pp. 1646–1651, 2011.

[32] S. S. Chen, "Roof control technology of fully mechanized coal mining face under special geological conditions," *Coal Science and Technology*, vol. 42, no. 2, pp. 124–128, 2014.

[33] G. L. Hui, S. J. Niu, H. W. Jing, and M. Wang, "Physical simulation on deformation rules of god-side roadway subjected to dynamic pressure," *Journal of Mining & Safety Engineering*, vol. 27, no. 1, pp. 77–86, 2010.

[34] P. Li, W. G. Qiao, and W. J. Song, "Analysis of settlement deformation laws of deep soft rock roadway," *Safety in Coal Mines*, vol. 47, no. 5, pp. 189–192, 2016.

[35] N. Cui, Z. G. Ma, D. W Yang et al., "Size optimization and energy analysis of coal pillar in the driving roadway along gob of the island coalface," *Journal of Mining & Safety Engineering*, vol. 34, no. 5, pp. 914–920, 2017.